

# Synthesis of $\text{MgAl}_2\text{O}_4$ spinel: seeding effects on formation temperature

J.-F. PASQUIER\*, S. KOMARNENI†, R. ROY

Materials Research Laboratory, The Pennsylvania State University, University Park, Pennsylvania 16802, USA

Four different methods of  $\text{MgAl}_2\text{O}_4$  spinel synthesis in the presence and absence of seeds were studied. The four methods used for  $\text{MgAl}_2\text{O}_4$  synthesis were (a) one sol (boehmite) and one solution [ $\text{Mg}(\text{NO}_3)_2$ ]; (b) two sols (boehmite and magnesia); (c) two nitrates (Al and Mg nitrates) and two alkoxides (Al isopropoxide and Mg ethoxide). The use of a nitrate route led to the formation of spinel at the lowest temperature without the influence of seeding. Seeding with spinel crystallites of all the powders except the one-sol and one-solution diphasic gels apparently resulted in a lower formation temperature of  $\text{MgAl}_2\text{O}_4$  spinel, and this lowering of crystallization temperature can be explained by the nucleation and epitaxial growth mechanism.

## 1. Introduction

The principle of structural diphasicity is based on the use of ultrafine seed crystals of the equilibrium phase in a non-crystalline gel. Since the concept was introduced, several compositional systems have been studied in our laboratory. The effects of seeding are significant in several systems such as  $\text{Al}_2\text{O}_3\text{-H}_2\text{O}$  [1-8],  $\text{MgO-Al}_2\text{O}_3$  [8-10],  $\text{Al}_2\text{O}_3\text{-SiO}_2$  [11, 12],  $\text{ZrO}_2\text{-SiO}_2$  [13] and  $\text{ThO}_2\text{-SiO}_2$  [14]. Crystallographic seeding was found to stabilize a particular phase or to lower the crystallization or formation temperature, and/or to enhance the densification.

Earlier work by Suwa *et al.* [8-10] on the system  $\text{Al}_2\text{O}_3\text{-MgO}$  with compositions 93.7 wt % and 95.2:4.8 wt % showed that isostructural seeding with the final equilibrium phases (i.e. spinel and  $\alpha\text{-Al}_2\text{O}_3$ ) resulted in enhanced densification upon sintering at lower temperatures. Moreover, microstructural characterization revealed uniform grain growth with little or no porosity in the gels with isostructural seeds, while non-uniform grain growth and porosity were seen in unseeded gels as well as in gels with non-isostructural seeds.

The objectives of our present work were to study the synthesis of  $\text{MgAl}_2\text{O}_4$  spinel using different routes and to investigate the effects of isostructural and non-isostructural seeding in this system. The  $\text{MgAl}_2\text{O}_4$  spinel is an interesting and very well known material which is mainly used as an abrasive material. It is also used as a substrate in phase-shifters [15].

## 2. Experimental procedure

### 2.1. Synthesis

#### 2.1.1. Sol-gel route 1 (one sol and one solution): boehmite and magnesium nitrate as starting materials

Diphasic xerogels of composition 50:50 mol % in the

$\text{Al}_2\text{O}_3\text{-MgO}$  system were prepared from boehmite (Dispural, Remet Chemical Corporation, Chadwicks, New York) and  $\text{Mg}(\text{NO}_3)_2 \cdot 6\text{H}_2\text{O}$  (Fisher Scientific, Fair Lawn, New Jersey). A magnesium nitrate solution (25 wt % in water) was made and added dropwise to clear boehmite hydrosol, which was prepared by initially dispersing boehmite in water (concentration 4.6 wt %) and subsequently adding 1N  $\text{HNO}_3$  dropwise while stirring [ $(\text{HNO}_3)/(\text{AlOOH}) = 0.06$ ]. The seed crystals, spinel (Baikalox SG, Baikowski International Corporation, Charlotte, North Carolina),  $\text{TiO}_2$  (anatase),  $\alpha\text{-Al}_2\text{O}_3$  (Baikalox CR6, Baikowski) or  $\gamma\text{-Al}_2\text{O}_3$  (GA-40, J. T. Baker Chemical Co., Phillipsburg, New Jersey) were peptized by  $\text{HNO}_3$  and added to the boehmite hydrosol before the addition of  $\text{Mg}(\text{NO}_3)_2$  solution. The amount of introduced seeds was, in all cases, 1.69 wt % of the expected spinel. The boehmite sol rapidly flocculated and gelled upon the addition of the magnesium nitrate. The gel was dried at 60 °C for 3 days, ground and calcined at 500 °C. The obtained powder was sintered at different temperatures in pellet form (with 1 wt % PVA) prior to characterization by different methods.

#### 2.1.2. Sol-gel route 2 (two sols): boehmite and MgO powder as starting materials

These diphasic nanocomposite xerogels were prepared from boehmite (Dispural) and MgO ultrafine powder (UC-999, UBE Industries, Ltd., Ube, Japan). The boehmite sol was prepared and seeded in much the same way as above, except with a boehmite concentration of 10 wt % and  $(\text{HNO}_3)/(\text{AlOOH})$  of 0.07. The MgO powder was dispersed in water (concentration 1.5 wt %) and slowly added to the boehmite hydrosol. The mixed sol, with a seed concentration of 1.69 wt %, rapidly flocculated and gelled. The gels were dried at

\* Visiting Scientist of Rhône-Poulenc, France.

† Also with the Department of Agronomy.

60 °C for 3 days, ground, calcined at 500 °C and sintered in pellet form (with 1 wt % PVA) before characterization by different methods.

### 2.1.3. Nitrates route (two nitrates): aluminum nitrate and magnesium nitrate as starting materials

Mg(NO<sub>3</sub>)<sub>2</sub>·6H<sub>2</sub>O (Fisher) and Al(NO<sub>3</sub>)<sub>3</sub>·9H<sub>2</sub>O (Aldrich Chemical Co., Milwaukee, Wisconsin) were mixed together with the minimum amount of water (concentration 65.5 wt %) and the seed crystals were added while stirring. The nitrate solution, with 1.69 wt % of seeds, was calcined at 600 °C for 2 h and the resulting powder was ground and sintered in pellet form (with 1 wt % PVA) at different temperatures. The characterization was carried out after sintering.

### 2.1.4. Alkoxides route (two alkoxides): aluminum isopropoxide and magnesium ethoxide as starting materials

Aluminum isopropoxide [Al(OC<sub>3</sub>H<sub>7</sub>)<sub>3</sub>] and magnesium ethoxide [Mg(OC<sub>2</sub>H<sub>5</sub>)<sub>2</sub>] (Aldrich) were dispersed in methanol (concentration: 12.6 wt %) in stoichiometric amounts to form the spinel MgAl<sub>2</sub>O<sub>4</sub>. The seed crystals (spinel, anatase, α-Al<sub>2</sub>O<sub>3</sub> and γ-Al<sub>2</sub>O<sub>3</sub>) were dispersed in methanol, CH<sub>3</sub>OH and added to the alkoxide dispersion in order to have a concentration of 1.69 wt % in seeds. The resulting mixture was heated at 80 °C by refluxing in air for 24 h and dried. After drying, the powder was calcined at 500 °C to remove all the organics. Pellets of the powder (with 1 wt % PVA) were pressed and sintered at different temperatures before characterization.

## 2.2. Characterization of materials

### 2.2.1. Particle size of precursor powders

The particle size of the precursor powders obtained by the different syntheses was determined using a Philips 420 transmission electron microscope (TEM). These powders were pelletized and heated in air using a programmed furnace (Lindberg, Watertown, Wisconsin). The heating rates were 1 °C min<sup>-1</sup> up to 200 °C (heated for 1 h at this temperature), 1.5 °C min<sup>-1</sup> between 200 and 500 °C, 3 °C min<sup>-1</sup> between 500 and 800 °C, and 10 °C min<sup>-1</sup> above 800 °C. The samples were heated for 100 min at the final sintering temperature. These temperatures were 800, 900, 1000, 1100 and up to 1200 °C in some cases. The apparent densities of the sintered materials after evacuation were measured by the Archimedes technique. The apparent density measured did not take open porosity into consideration. Microstructures of the fractured pellets were observed by scanning electron microscope (SEM) using an ISI DS 130 instrument.

### 2.2.2. Characterization of the spinel phase by qualitative and quantitative X-ray diffraction

X-ray powder diffraction was carried out on samples

heated to various temperatures with a Scintag Pad-V diffractometer, using nickel-filtered CuK<sub>α</sub> radiation.

Before crystallization of a pure spinel in the system MgO–Al<sub>2</sub>O<sub>3</sub>, a stabilized γ-Al<sub>2</sub>O<sub>3</sub>–MgAl<sub>2</sub>O<sub>4</sub> solid solution is formed, and its formation is in competition with that of the MgAl<sub>2</sub>O<sub>4</sub> spinel phase. The X-ray diffraction patterns of MgAl<sub>2</sub>O<sub>4</sub> (PDF No. 21-1152) and of γ-Al<sub>2</sub>O<sub>3</sub> (PDF No. 11-0425) are very similar, and the major peaks merge. The most intense peaks (*I* = 100%) for the MgAl<sub>2</sub>O<sub>4</sub> spinel and γ-Al<sub>2</sub>O<sub>3</sub> are the 311 *hkl* reflection (*d* = 0.244 nm) and the 400 *hkl* reflection (*d* = 0.198 nm), respectively. However, the 400 *hkl* peak of the MgAl<sub>2</sub>O<sub>4</sub> spinel (*d* = 0.202 nm) and the 311 *hkl* peak of γ-Al<sub>2</sub>O<sub>3</sub> (*d* = 0.239 nm) represent only 60% and 80%, respectively, of the most intense peaks.

Thus the formation of pure spinel or its solid solution with γ-Al<sub>2</sub>O<sub>3</sub> can be characterized by the relative intensity of the 311 and 400 peaks from the X-ray patterns of powders:

$$X = \frac{I_{(400)}}{I_{(311)}}$$

where *I*<sub>(400)</sub> is the intensity of the 400 (*hkl*) peak and *I*<sub>(311)</sub> is the intensity of the 311 (*hkl*) peak.

A pure crystal of spinel should have *X* = 60:100 = 0.60. If *X* > 0.60, it is assumed here to have a solid solution of γ-Al<sub>2</sub>O<sub>3</sub> and MgAl<sub>2</sub>O<sub>4</sub>. The parameter *X* will characterize the transformation of the solid solution to the pure spinel phase. Curves *X* against *T*, the pellet firing temperature, were used to compare the formation of MgAl<sub>2</sub>O<sub>4</sub> spinel for the four synthesis methods without and with seeds.

## 3. Results and discussion

### 3.1. Particle size and characteristics of the different spinel precursor powders (TEM observations)

TEM observations of the different powders showed some morphological differences of powders among the various routes (Fig. 1). Sol-gel 1 (Fig. 1a) and nitrates (Fig. 1c) routes led to fibres or rolled foils (100–200 nm long and 10–20 nm wide for sol-gel 1, and up to 100 nm long and 10 nm wide for the nitrates routes). The powder obtained from the alkoxides route (Fig. 1d) showed mainly foils (50 × 50 nm and 1 nm thick) with some grains of 5 nm. On the other hand, the sol-gel route 2 powder is a nanocomposite of two types of grains (5–50 nm) (Fig. 1b).

### 3.2. Formation of the spinel MgAl<sub>2</sub>O<sub>4</sub>: X-ray study

The curves *X* = *I*<sub>(400)</sub>/*I*<sub>(311)</sub> against *T*, the firing temperature, allow us to see some differences between the different synthesis methods and seedings. The sol-gel 1 route (Fig. 2) showed no significant differences without and with seeds, and the curves overlapped with each other. With the sol-gel 1 method, *X* is very high (up to 1000 °C) and reached 0.60 (the pure spinel *X* value) at 1100 °C. Even at this temperature, traces of the γ-Al<sub>2</sub>O<sub>3</sub>–MgAl<sub>2</sub>O<sub>4</sub> solid solution were still found

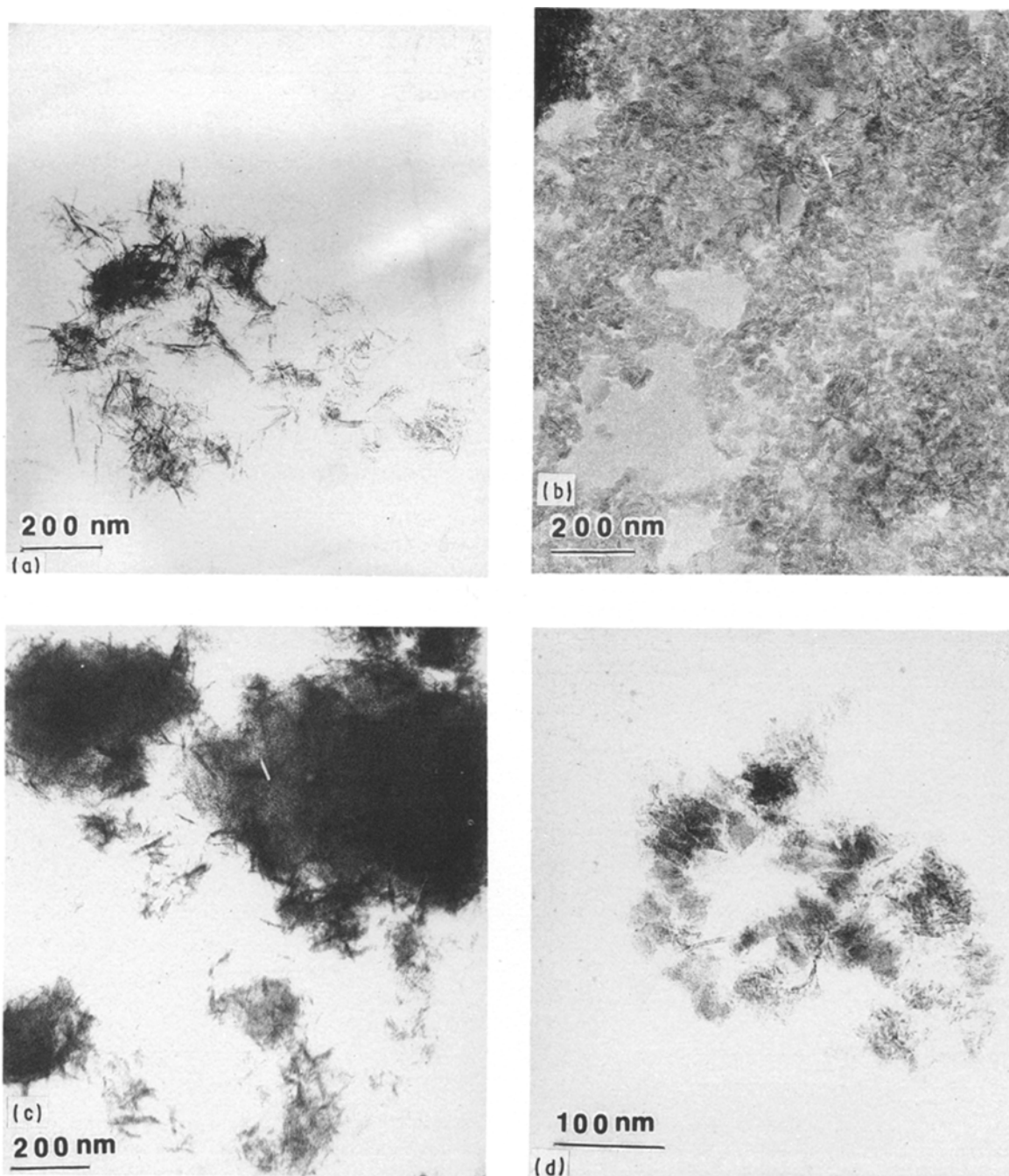


Figure 1 TEM micrographs of precursor  $\text{MgAl}_2\text{O}_4$  powders before heat treatment: (a) sol-gel route 1; (b) sol-gel route 2; (c) nitrates route; (d) alkoxides route.

(Table I) and this incomplete reaction may be attributed to inhomogeneous mixing of the two components in this method. On the other hand, the other three routes (see Figs 3–5) showed some effect of  $\text{MgAl}_2\text{O}_4$  seeding on the formation of  $\text{MgAl}_2\text{O}_4$ . The sol-gel 2 (Fig. 3) and alkoxides (Fig. 4) routes show well-separated curves, which indicates some seeding effect. Spinel seeding decreased  $X$  and enhanced the percentage of spinel at low temperatures, while the other seeds appear to have a slightly negative effect. But the alkoxides method showed a minor amount of  $\gamma\text{-Al}_2\text{O}_3\text{-MgAl}_2\text{O}_4$  solid solution even at  $1100^\circ\text{C}$  (Table I) and this shows that atomic-scale mixing was not achieved here, probably because of the different

hydrolysis rates of the two alkoxides. In the sol-gel 2 case, the spinel seeding decreased the value of  $X$  and this curve is similar to that obtained with the nitrates route (Fig. 5). It appears that more spinel had formed at low temperatures with the spinel seeding in the case of sol-gel route 2. The other seeds seem to have no effect ( $\gamma\text{-Al}_2\text{O}_3$ ) or a slightly negative effect (anatase and  $\alpha\text{-Al}_2\text{O}_3$ ).

The nitrates route showed  $X$  values which are close to 0.60 even at  $900^\circ\text{C}$ . Spinel  $\text{MgAl}_2\text{O}_4$  without  $\gamma\text{-Al}_2\text{O}_3$  in solid solution formed much earlier in the nitrates case, because of the atomic-scale mixing (Table I), and also exhibits a significant  $\text{MgAl}_2\text{O}_4$  spinel seeding effect for the same reason.

TABLE I Detected phases by X-ray diffraction and lattice parameter  $a_0$  of the spinel after heat treatment of pellets at 1100 °C for 100 min<sup>a</sup>

Route	Seeds	Detected phases	$a_0$ (nm)
Sol-gel 1	No seed	Spinel, MgO (traces)	0.80707
	Spinel	Spinel	0.80779
	TiO <sub>2</sub>	Spinel + $\gamma$ -Al <sub>2</sub> O <sub>3</sub> , MgO	0.80811
	$\alpha$ -Al <sub>2</sub> O <sub>3</sub>	Spinel, $\alpha$ -Al <sub>2</sub> O <sub>3</sub> , MgO	0.80827
	$\gamma$ -Al <sub>2</sub> O <sub>3</sub>	Spinel + $\gamma$ -Al <sub>2</sub> O <sub>3</sub> (traces)	0.80827
Sol-gel 2	No seed	Spinel	0.80799
	Spinel	Spinel	0.80559
	TiO <sub>2</sub>	Spinel	0.80547
	$\alpha$ -Al <sub>2</sub> O <sub>3</sub>	Spinel	0.80783
	$\gamma$ -Al <sub>2</sub> O <sub>3</sub>	Spinel	0.80772
Nitrates	No seed	Spinel	0.80927
	Spinel	Spinel	0.80791
	TiO <sub>2</sub>	Spinel	0.80807
	$\alpha$ -Al <sub>2</sub> O <sub>3</sub>	Spinel, $\alpha$ -Al <sub>2</sub> O <sub>3</sub> , MgO	0.80827
	$\gamma$ -Al <sub>2</sub> O <sub>3</sub>	Spinel	0.80871
Alkoxides	No seed	Spinel + $\gamma$ -Al <sub>2</sub> O <sub>3</sub> (traces), MgO (traces)	0.80799
	Spinel	Spinel + $\gamma$ -Al <sub>2</sub> O <sub>3</sub> , MgO	0.80807
	TiO <sub>2</sub>	Spinel + $\gamma$ -Al <sub>2</sub> O <sub>3</sub> , MgO	0.80847
	$\alpha$ -Al <sub>2</sub> O <sub>3</sub>	Spinel + $\gamma$ -Al <sub>2</sub> O <sub>3</sub> , $\alpha$ -Al <sub>2</sub> O <sub>3</sub> , MgO	0.80819
	$\gamma$ -Al <sub>2</sub> O <sub>3</sub>	Spinel + $\gamma$ -Al <sub>2</sub> O <sub>3</sub> , $\alpha$ -Al <sub>2</sub> O <sub>3</sub> , MgO	0.80855

<sup>a</sup> Theoretical lattice parameter of spinel MgAl<sub>2</sub>O<sub>4</sub> = 0.80831 (PDF 21-1152); theoretical lattice parameter of  $\gamma$ -Al<sub>2</sub>O<sub>3</sub> = 0.790 (PDF 10-425).

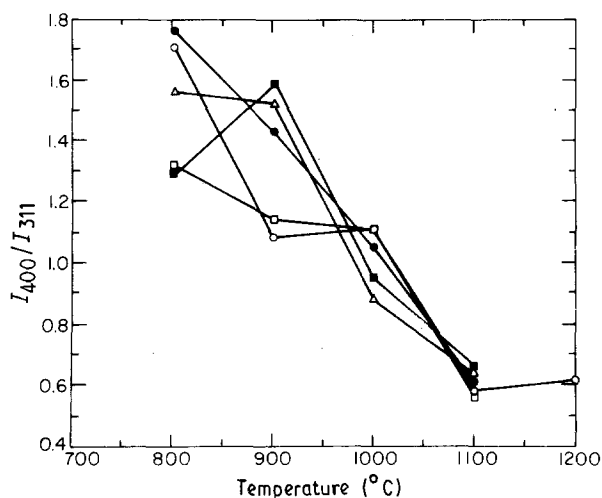


Figure 2  $X = I_{400}/I_{311}$  against  $T$ , firing temperature, for sol-gel route 1 with and without seeds.  $\square$ , No seed;  $\bullet$ , spinel seeds;  $\Delta$ , anatase seeds;  $\circ$ ,  $\alpha$ -Al<sub>2</sub>O<sub>3</sub> seeds;  $\blacksquare$ ,  $\gamma$ -Al<sub>2</sub>O<sub>3</sub> seeds.

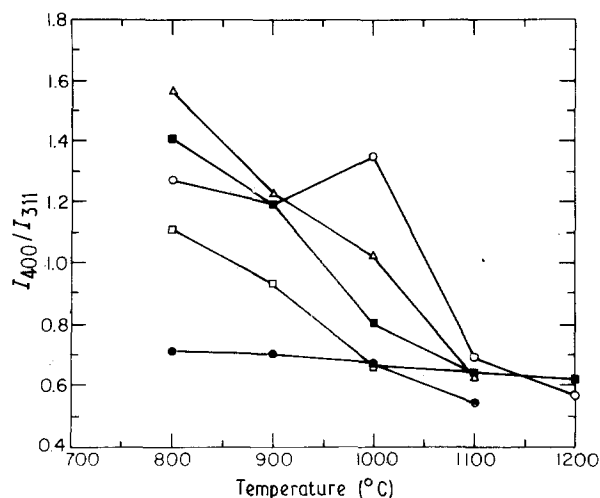


Figure 4  $X = I_{400}/I_{311}$  against  $T$ , firing temperature, for alkoxides route with and without seeds.  $\square$ , No seed;  $\bullet$ , spinel seeds;  $\Delta$ , anatase seeds;  $\circ$ ,  $\alpha$ -Al<sub>2</sub>O<sub>3</sub> seeds;  $\blacksquare$ ,  $\gamma$ -Al<sub>2</sub>O<sub>3</sub> seeds.

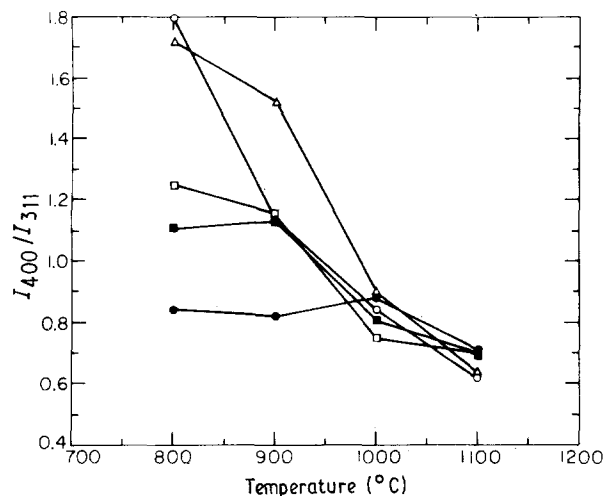


Figure 3  $X = I_{400}/I_{311}$  against  $T$ , firing temperature, for sol-gel route 2 with and without seeds.  $\square$ , No seed;  $\bullet$ , spinel seeds;  $\Delta$ , anatase seeds;  $\circ$ ,  $\alpha$ -Al<sub>2</sub>O<sub>3</sub> seeds;  $\blacksquare$ ,  $\gamma$ -Al<sub>2</sub>O<sub>3</sub> seeds.

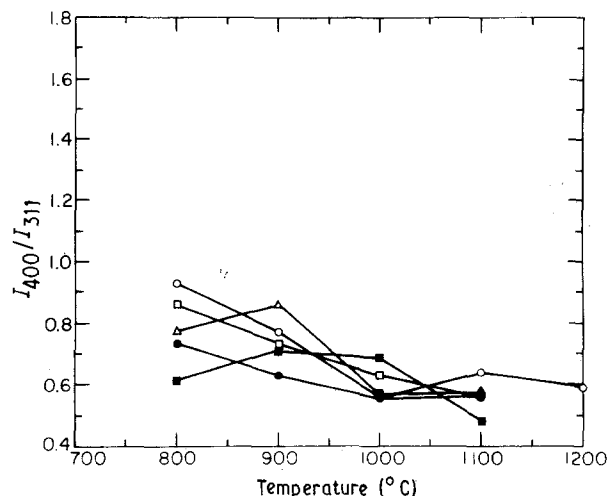


Figure 5  $X = I_{400}/I_{311}$  against  $T$ , firing temperature, for nitrates route with and without seeds.  $\square$ , No seed;  $\bullet$ , spinel seeds;  $\Delta$ , anatase seeds;  $\circ$ ,  $\alpha$ -Al<sub>2</sub>O<sub>3</sub> seeds;  $\blacksquare$ ,  $\gamma$ -Al<sub>2</sub>O<sub>3</sub> seeds.

### 3.3. Densification of $\text{MgAl}_2\text{O}_4$ prepared by different methods

Pellets of  $\text{MgAl}_2\text{O}_4$  made from different methods showed high apparent densities (Table II), but the microstructure of fractured surfaces (Fig. 6) shows substantial porosity and an ultrafine crystal size. Although bulk densities were not measured here, the micrographs clearly show that these pellets have a low bulk density. The large difference between the appar-

TABLE II Apparent densities, relative to theoretical density of spinel (3.5782), of pellets of  $\text{MgAl}_2\text{O}_4$  synthesized by different methods

Method of synthesis	Apparent density ( $\text{g cm}^{-3}$ ) after sintering at 1100 °C for 100 min
Sol-gel route 1	97.1
Sol-gel route 2	98.4
Alkoxides route	96.1
Nitrates route	97.2

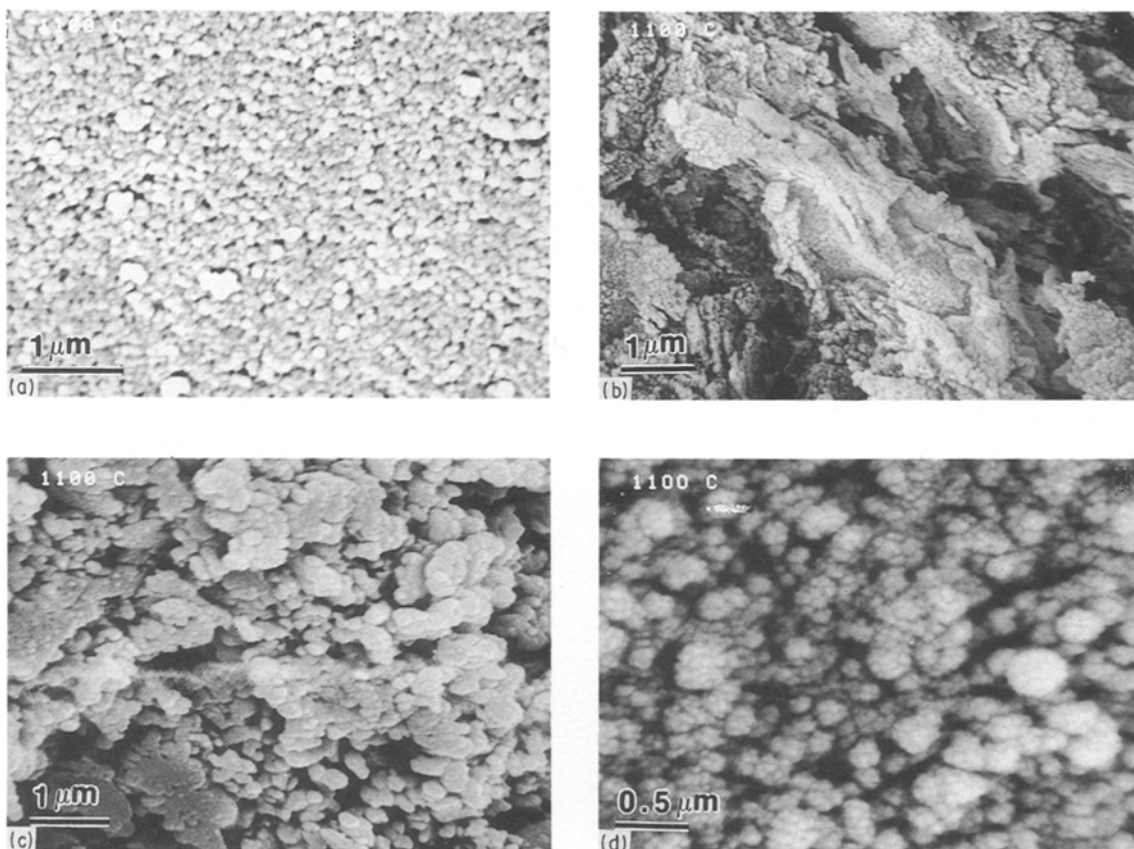


Figure 6 SEM micrographs of  $\text{MgAl}_2\text{O}_4$  pellets (fractured surfaces), sintered at 1100 °C, prepared by (a) sol-gel route 1; (b) sol-gel route 2; (c) nitrates route; (d) alkoxides route.

ent and bulk densities points to an interconnected porosity in these  $\text{MgAl}_2\text{O}_4$  samples, and these samples may be useful as ceramic membranes for high-temperature separations.

### 4. Conclusions

Isostructural seeding of  $\text{MgAl}_2\text{O}_4$  composition powders led in general to a decrease in the crystallization temperature of  $\text{MgAl}_2\text{O}_4$  spinel which can be attributed to the nucleation and epitaxial growth mechanism.

### Acknowledgements

This research was supported by the National Science Foundation under Grant No. DMR-8507912. Jean-François Pasquier would like to thank Rhône-

Poulenc for its financial support of his tenure at the University. The authors thank Else Breval for her help with the TEM observations.

### References

1. M. KUMAGAI and G. MESSING, *J. Amer. Ceram. Soc.* **67** (1984) C-230.
2. *Idem.*, *ibid.* **68** (1985) 500.
3. R. A. SHELLEMAN, G. L. MESSING and M. KUMAGAI, *J. Non-Cryst. Solids* **82** (1986) 277.
4. G. MESSING, J. L. McARDLE and R. A. SHELLEMAN, *Mater. Res. Soc. Symp. Proc.* **73** (1986) 71.
5. W. A. YARBROUGH and R. ROY, *Nature* **322** (1986) 347.
6. *Idem.*, *J. Mater. Res.* **2** (1987) 494.
7. Y. SUWA, S. KOMARNENI and R. ROY, *J. Mater. Sci. Lett.* **5** (1986) 21.
8. R. ROY, Y. SUWA and S. KOMARNENI, in "Science of Ceramic Chemical Processing", edited by L. L. Hench and D. R. Ulrich (Wiley, New York, 1986) p. 247.
9. Y. SUWA, R. ROY and S. KOMARNENI, *Mater. Sci. Engng* **83** (1986) 151.
10. *Idem.*, *J. Amer. Ceram. Soc.* **68** (1985) C-238.
11. D. W. HOFFMAN, R. ROY and S. KOMARNENI, *ibid.* **67** (1984) 468.

12. T. J. MROZ and J. LAUGHNER, presented at the American Ceramic Society 40th Pacific Coast Regional Meeting (1987).
13. G. VILMIN, S. KOMARNENI and R. ROY, *J. Mater. Sci.* **22** (1987) 3556.
14. *Idem.*, *J. Mater. Res.* **2** (1987) 489.

15. M. SUGIURA and O. KAMIGAITO, *Yogyo-Kyokai-Shi* **92** (1984) 605.

*Received 13 March  
and accepted 4 September 1990*